Mixed metal oxide: A new class of catalyst for methanol activation

Shweta Mehta[a,c,1], Sheena Agarwal[a,c,1], Nivedita Kenge[a,c], Siva Prasad Mekala[b], Vipul Patil[b], T. Raja[b,c], Kavita Joshi[a,c]

[a] *Physical and Materials Chemistry Division, CSIR-National Chemical Laboratory, Dr. Homi Bhabha Road, Pashan, Pune 411008, India*
[b] *Catalysis Division, CSIR-National Chemical Laboratory, Dr. Homi Bhabha Road, Pashan, Pune 411008, India*
[c] *Academy of Scientific and Innovative Research (AcSIR), Anusandhan Bhawan, 2, Rafi Marg, New Delhi 110001, India*

ARTICLE INFO

ABSTRACT

In this work, we propose a mixed metal oxide as a catalyst and demonstrate it's ability to not only activate the MeOH molecule upon adsorption but also dissociate O−H and one of it's C−H bonds. MeOH activation is compared on two prominent facets of ZnAl₂O₄ viz. (2 2 0) and (3 1 1). While spontaneous O−H bond dissociation is observed on both facets, C−H bond dissociates only on the (3 1 1) surface. Multiple factors like atomic arrangement and steps on the surface, coordination of surface atoms, and their effective charges have a combined effect on MeOH activation. The (3 1 1) surface offers higher catalytic activity in comparison with (2 2 0) surface. Having a stepped surface, availability of multiple sites, and variation in the charge distribution are some of the reasons for better catalytic performance of (3 1 1) facet. Effect of orientation of MeOH with respect to the surface adds both, information and complexity to the problem. Observations pertinent to understanding this effect are also reported. A detailed analysis of atomic arrangement on the two surfaces provides a rationale as to why MeOH gets dissociated spontaneously on the mixed metal oxide. The promising results reported here opens up a new class of catalyst for research.

1. Introduction

Methanol (MeOH), the simplest aliphatic alcohol is a commodity chemical and produced in large quantities. It is used in production of many hydrocarbons like gasoline, olefins, as well as chemicals such as formaldehyde, dimethyl ether to name a few [1,2]. It is also being considered as a source of fuel in direct methanol fuel cells [3,4]. Irrespective of the end product, conversion of MeOH requires one or more of O−H, C−H, and/or C−O bond activation and hence its adsorption and decomposition has been studied extensively by both experimental [5–15] as well as theoretical means [16–29]. Amount of activation in terms of either binding energies or bond lengths, activation barriers for O−H or one of the C−H bond scission along with factors influencing the activation are investigated in these studies. Activation of methanol over different types of materials like transition metal surfaces [30–41], metal clusters [8,34,42,43], binary metal alloys [44,45,43,46–50], metal oxides [20,50–65], and zeolites [28,29] is studied extensively. Among the various studies on transition metal surfaces, enhanced MeOH activation and hence lowered activation barriers are reported on surfaces with preadsorbed oxygen [31,32].

Methanol activation is also investigated theoretically on various binary metal alloys like CoPt [44,45], NiPt [47], NiAl [43,46], PdZn [50] etc. In a combined experimental and theoretical study, Skoplyak et. al. investigates methanol reactivity trends on bimetallic surfaces like NiPt(1 1 1) and CoPt(1 1 1). Their results reveal an interesting correlation between the methanol and methoxy binding energies, and the d-band center of various NiPt(1 1 1) and CoPt(1 1 1) bimetallic surfaces [44]. In an another interesting study, Lawrence et. al. demonstrate the C−O bond weakening over NiAl(1 0 0) facet which leads to ejection of the methyl group from methanol [43]. Du et. al. report that on Pt₃Ni (1 1 1), less electronegative Ni atoms are more favorable for adsorbing radical intermediates and intermediates with lone-pair electrons (such as O-containing species). They also conclude that out of the possible bond scissions, O−H bond scission is the most favorable [47]. In a study by Smith et. al., a detailed analysis of MeOH activation and different pathways through which it can undergo dissociation is reported on various PdZn facets [50]. Their calculations indicate that the dissociation of both methanol and water is highly activated on flat surfaces of PdZn such as (1 1 1) and (1 0 0), while the dissociation barriers can be lowered significantly by surface defects, like (2 2 1), (1 1 0), and (3 2 1) faces of PdZn.

Due to presence of both acidic and basic sites on metal oxide

---

surfaces, they are considered to be more efficient for wide variety of catalytic reactions. MeOH adsorption has also been studied on various metal oxide surfaces such as CeO_2 [20], MgO [42,51,64,65], Cr_2O_3 [52], Cu_2O [53], TiO_2 [54,55], Al_2O_3 [18,52,56], ZnO [50,57], β-Ga_2O_3 [58], etc. Riguang et. al. highlight the role of preadsorbed oxygen on Cu_2O (1 1 1) surface in O−H bond dissociation [53]. Their DFT based calculations show that the O−H bond dissociation path has the lowest activation barrier 0.28 eV. Oxygen-precovered Cu_2O (1 1 1) surface exhibits high surface reactivity towards the formation of CH_3O^- by the O−H bond-cleavage, and reduces the activation barrier for O−H bond cleavage. For activation of methanol over MgO surfaces, Branda et. al. explains the important role of coordination numbers for reactivity of adsorbate. They report that oxide surface atoms with different co-ordination numbers show very different reactivity giving both molecular and dissociated adsorbed species [42,64,65]. Recent study by Liu et. al. reports spontaneous dissociation of methanol over CeO_2 (1 1 0) facet. Further, dissociation on the (1 1 0) surface of CeO_2 is site selective and dissociation does not occur at all on the (1 1 1) surface, where only physisorption was found. Their analysis of surface geometries shows that dominant factors for the dissociation of methanol are under-coordinated surface atoms with their varying charges [61].

Today, ZnO/Al_2O_3 catalysts are the most relevant industrial catalyst for methanol synthesis. DFT based studies in this direction are geared to understand the surface chemistry [18,50,52,56,57]. In a study, Borck et. al. show that while methanol adsorption is not dissociative on α-Al_2O_3 (0 0 0 1) in the absence of co-adsorbed H atoms, their results for methanol adsorption on α-Cr_2O_3 (0 0 0 1) indicate that dissociation may take place to obtain the energetically preferred methoxy adsorption [52]. In another study by the same group, adsorption of methanol on Al_2O_3 surface is shown to have maximum O−H bond elongation up to 1.02 Å. They also studied the decrease in the adsorption energy with increasing monolayer coverage of methanol on the surface [18]. In yet another study catalytic dehydration of methanol to dimethyl ether over modified γ-Al_2O_3 with Nb_2O_5 catalysts were investigated [56]. The conversion of methanol was reported to be enhanced due to Nb_2O_5 modification as it increased the number and reduced the strength of these acidic sites at lower temperatures. Vo et. al. studied the adsorption and decomposition of methanol on ZnO (1 0 1 0) surface. The O−H bond of MeOH elongates up to 1.05 Å. The MeOH dehydrogenation to methoxy has an activation barrier of 0.56 eV and subsequent dehydrogenation of methoxy to formaldehyde has an activation barrier of 1.20 eV [57]. Smith et. al. report an activation barrier of 0.39 eV for dissociation of methanol over defect free polar ZnO(0 0 0 1) surface [50].

As we have discussed, MeOH activation is extensively studied on metals, binary alloys as well as metal oxide surfaces by employing DFT based computation. However, to the best of our knowledge, MeOH activation on a mixed metal oxide is not yet studied. In the present work we investigate the nature of interaction between a methanol molecule and a mixed metal oxide prepared by combining Al_2O_3 and ZnO to form $ZnAl_2O_4$. We demonstrate that activation as well as spontaneous dissociation of O−H and one of it's C−H bonds takes place on this mixed metal oxide catalyst. Study of MeOH activation on (3 1 1) and (2 2 0) surfaces of $ZnAl_2O_4$ were chosen particularly because their stability has been confirmed in XRD peaks [66–70]. Overall, it was observed that both surfaces offer sites that activate as well as dissociate O−H bond in MeOH. Adsorption and activation of O−H bond was observed with varying strengths on both surfaces. (3 1 1) in particular proved to offer greater catalytic activity than (2 2 0). Not only O−H but also C−H bond dissociation was observed on (3 1 1) surface.

2. Computational details

All the calculations were carried out within the Kohn-Sham formalism of density functional theory (DFT). Projector Augmented Wave potential [71,72] was used, with Perdew Burke Ehrzenhof (PBE)[73]

approximation for the exchange-correlation and generalized gradient approximation, [74] as implemented in planewave, pseudopotential based code, Vienna Ab initio Simulation Package (*VASP*) [75–77]. The bulk unit cell was taken from the materials project [78] and optimized. The bulk lattice constant without applying DFT + U correction is 8.0640 Å which is in excellent agreement with the experimentally measured lattice parameter 8.0779 Å [70]. Two different facets, (2 2 0) and (3 1 1) of $ZnAl_2O_4$ were modeled as slab by cleaving a surface with 4 layers in 220 (3 1 1) direction with pymatgen [79]. Van der Waals corrections were applied to all the calculations. The vacuum along z-axis which is also adjusted as 220 (3 1 1) direction of the crystal, was varied from 15 Å till 25 Å with the step of 2.5 Å. It was found that 20 Å of vacuum was sufficient to avoid interaction between adjacent images of planes along the z-direction. Geometry optimization was carried out with a force cutoff of 0.05 eV/Å on the unfixed atoms and the total energies were converged below 10^{-4} eV for each SCF cycle. A Monkhorst-Pack grid of 6x4x1 was used which resulted into 12 k-points in IBZ to emulate the solid slab. Entire surface was scanned by placing the MeOH molecule at unique available sites. To compare the adsorption on these sites, adsorption energy was calculated using the formula: $E_{ads} = E_{system} - E_{surface} - E_{molecule}$ where E_{system} is energy of the system when MeOH is placed on the surface, $E_{surface}$ is energy of the bare surface and $E_{molecule}$ is energy of the MeOH molecule. To understand the site specific adsorption pattern, the site-dependent projected Density of States (*pDOS*) were calculated with denser k-mesh using LOBSTER [80–83]. Mulliken charges were calculated for all the atoms on the surface which provided insights about the quantitative charge transfer.

3. Results and discussion

$ZnAl_2O_4$ is a normal spinel metal oxide with a cubic lattice and $Fd\bar{3}m$ space group [84]. In this spinel compound, oxide ions occupy the Wyckoff position and form a face-centered cubic sublattice where Zn^{+2} ions occupy tetrahedral sites while Al^{+3} occupy octahedral sites. These Zn^{+2} ions are coordinated with four nearest neighbor oxygens whereas the Al^{+3} ions have six oxygen atoms as their nearest neighbors in the bulk structure. In case of $ZnAl_2O_4$, since the surface is polar, it could be terminated in two different ways, and it has been demonstrated that AlO_2 terminated surface is favored over $ZnAlO_2$ termination [85]. (2 2 0) and (3 1 1) are the most prominent peaks in the XRD pattern of $ZnAl_2O_4$ and hence we have chosen to study these surfaces for MeOH adsorption [66–70].

3.1. Interaction of MeOH with $ZnAl_2O_4$ (2 2 0) surface

The (2 2 0) is flat and comparatively more symmetric than a stepped surface and is shown in Fig. 1. Since, it is a polar surface, it can be terminated in two different ways, through AlO_2 or $ZnAlO_2$. We model the AlO_2 termination, where the top most layer of the surface is rich in Al and O atoms. Zn atoms are present in the subsurface layer and are not available to act as an active site for adsorption of an incoming MeOH molecule. As will be explained in detail later, the relative arrangement of atoms on the surface changes the environment that an incoming adsorbate experiences. The nature of bonding is hence influenced due to the changing surface catalyst environment.

As a first step towards understanding MeOH adsorption on this facet, most favored orientation of MeOH was investigated by studying it's adsorption through C, O, H_{OH} (H attached to O in MeOH) and H_{CH} (H attached to C in MeOH). When MeOH is placed through carbon or H_{CH} on the surface, the molecule does not adsorb thus indicating that these are the unfavored orientations for adsorption. When MeOH is placed through oxygen or H_{OH} on the surface, the molecule changes its orientation and adsorbs with its oxygen atom pointing towards the surface. Thus, the most favorable orientation of MeOH is when it adsorbs via its oxygen atom and all the initial configurations hence forth have MeOH placed by pointing its oxygen towards the surface.
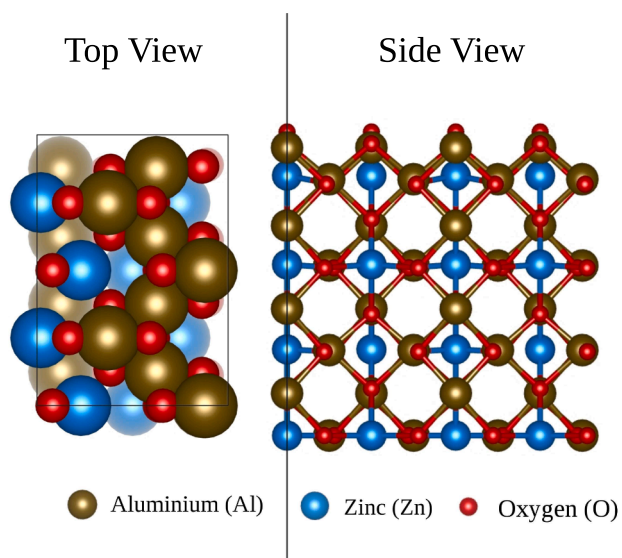
Top View

Side View

● Aluminium (Al) ● Zinc (Zn) ● Oxygen (O)

Fig. 1. The (2 2 0) surface of ZnAl$_2$O$_4$ with the top view and the side view. The top-most layer of (2 2 0) surface consist of Al and O atoms.

However, let's note that even this favorable position of MeOH can have many relative orientations wrt surface atoms as shown in Fig. 2 which leads to the variation in adsorption energy for the same adsorption site. Fig. 2 explains manifold possibilities that exist due to the relative orientation of MeOH wrt the surface. Rotation around the normal to the surface (N$_{surf}$), change in the angle between N$_{surf}$ and OC axis of MeOH, and rotation around OC axis of the MeOH results into many possibilities in which a molecule can interact with the surface when placed at a specific site. In all these cases, change in the relative orientation of MeOH wrt surface will affect the interaction between surface and MeOH. The effect of this relative orientation is explained in detail later and it turns out to be an important factor in understanding adsorption energy as well as bond activation trends.

All the unique sites are scanned on (2 2 0) surface by placing MeOH through O. This includes on top sites of Al as well as subsurface Zn, various bridge sites between Al−Al, Al−Zn, Al−O, Zn−O as well as

hollow positions. All these sites where MeOH was placed as starting configuration are shown schematically in Fig. 3-a and the final positions of MeOH upon adsorption are shown in Fig. 3-b. As Fig. 3-b indicates MeOH adsorbs on surface Al in most of the cases. However, there are few cases where it also gets adsorbed on a bridge or at a hollow position. We report the adsorption energies E$_{ads}$, O−H bond activation, metal-O$_{MeOH}$ (O of MeOH) distance and H$_{OH}$-O$_{surf}$ (surface oxygen) distances in Table 1. The observation table is divided in three parts based on the amount of activation O−H bond undergoes and adsorption site. It was observed that the trends in the activation of the O−H bond could be understood if we systematically investigate the nearby environment of the adsorption site. The first class comprises of cases where the O−H bond in methanol was barely activated from 0.97 Å to 0.98–1.00 Å. The second class includes all cases for which the O−H bond activation was greater than 1.00 Å, i.e. between 1.01 Å to 1.04 Å. An important observation made during the adsorption studies was that irrespective of initial orientation of O−H bond, finally the bond would orient itself such that the H$_{OH}$ would face nearest surface oxygen. The entire molecule gets stably adsorbed on top of the nearest Al atom reorienting its H facing the nearby surface oxygen. This observation can also be realized by investigating the H$_{OH}$-O$_{surf}$ distances in Table 1. For cases where O−H bond activation is not more than 4–5% (class I) the distance of O$_{surf}$ from H$_{OH}$ is in the range of 1.74 Å to 2.12 Å. Whereas for the class II cases, with an activation up to 7–9%, the distance between H$_{OH}$ and O$_{surf}$ reduces to 1.52 Å–1.67 Å. The proximity of surface oxygen atom and reorientation of O−H bond explains the trends in OH bond activation of methanol over the surface.

The adsorption energies for most of the cases in these two classes also follow a trend wherein overall adsorption energies for class II are more than that of class I. The third class of cases, i.e. positions 9, 7, and 6, are the ones that do not adsorb directly on top on any surface atom, but rather adsorb on either a hollow site or a bridge site. As it can be seen from Fig. 3(b), there is no Al atom directly below the adsorbed methanol. But the presence of nearby oxygen atom on surface interacts with the H from methanol leading to the O−H bond activation, as can be seen from Table 1.

Although we have scanned almost all the unique "sites" on the surface (taking into account symmetry), scanning all possible orientations of MeOH molecule wrt to a specific site is a formidable task and
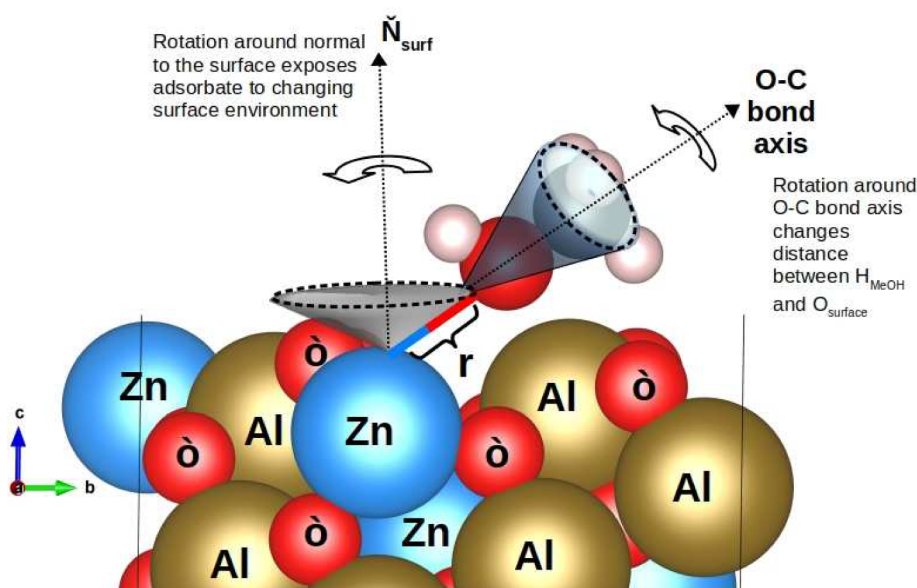

Fig. 2. Figure explains the large number of possibilities due to relative orientation of MeOH wrt the surface. Rotation around the normal to the surface, varying angle between N$_{surf}$ and OC axis of MeOH and rotation around OC axis of the MeOH results into large number of possibilities in which molecule can interact with the surface when placed at a specific site.
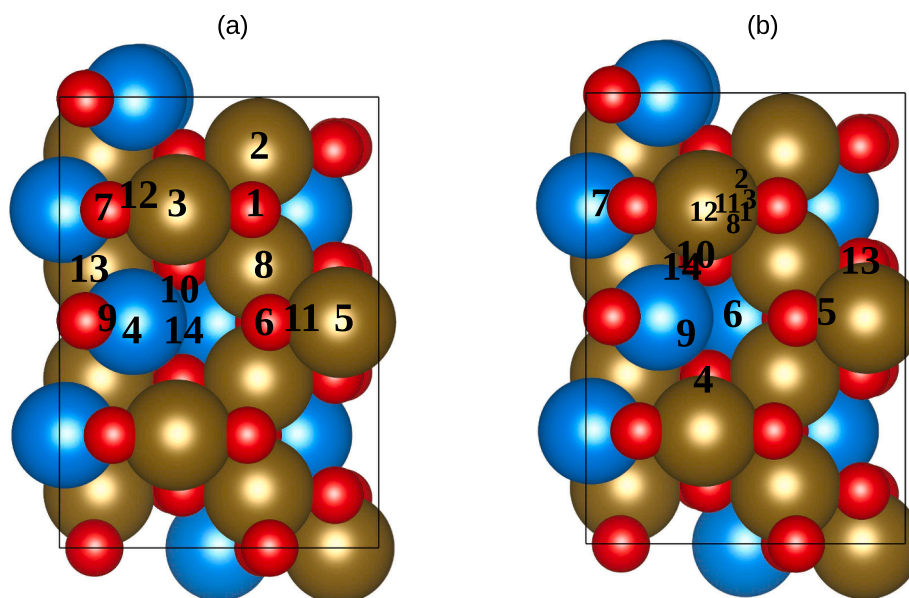
Fig. 3. The (2 2 0) surface of ZnAl$_2$O$_4$ shows (a) initial positions of adsorbate on the surface (b) final positions of methanol upon relaxation. It could be seen that in most of the cases irrespective of the initial position, MeOH adsorbs on surface Al.

Table 1
Adsorption energies, O−H bond activation, distance between O$_{OH}$ and surface metal (M) atom, and H$_{OH}$-O$_{surf}$ distance for adsorption studied at various positions as indicated in Column 1 on (2 2 0) (refer to Fig. 3 for site specifications).

Adsorption Site	E_{ads} (eV)	O−H Bondlengths (Å)	O−Al distance (Å)	H$_{(MeOH)}$ − O$_{surface}$ distance (Å)
		Class I - Barely activated		
4	− 1.5459	1.01	1.96 -Al	1.74
8	− 1.3590	1.00	1.92 -Al	1.75
2	− 1.3754	1.00	1.92 -Al	1.76
11	− 1.3262	1.00	1.90 -Al	1.78
3	− 1.3582	0.99	1.91 -Al	1.94
12	− 1.3751	0.98	1.92 -Al	2.12
		Class II - Moderately activated		
1	− 1.2636	1.04	1.87 -Al	1.52
14	− 1.5687	1.02	1.96 -Al	1.66
10	− 1.5590	1.02	1.96 -Al	1.67
		Class III - Adsorbed on bridge/hollow		
9	− 0.6603	1.01	3.62 -Zn	1.64
7	− 0.6099	1.00	3.99 -Zn	1.69
6	− 0.4977	0.99	4.14 -Al	2.04

still not achieved. However, to bring out the effect of "change in orientation" on the adsorption of MeOH, we have added all the distinct cases where molecule was adsorbed on the surface. This includes cases like MeOH adsorbed at same site but having different orientations. For example, in Fig. 4, MeOH is placed at 12th and 14th positions on (2 2 0) surface and share a common adsorption site (refer Fig. 3-b). The Al−O bond distance is nearly same in both the cases as noted in the Fig. 4. Further, the difference in adsorption energies is also less than 1 meV. However, the O−H bond activation is 0.98 Å (barely activated) in case of 12th position whereas 1.02 Å (moderately activated) in case of 14th position. And this can be directly understood if we look at the H$_{MeOH}$-O$_{surf}$ distances. This brings out the effect of orientation of the molecule on adsorption. Over the same adsorption site, it could change the surface environment experienced by atoms in the molecule and hence the resultant interaction and activation. This is applicable to molecule at position 8 and 3 in class I of (2 2 0) surface as well.

Finally, we report the case wherein O−H bond dissociation is observed, i.e. when placed at position 13 and is shown in Fig. 5. This is an

important case as it represents spontaneous dissociation of O−H bond in methanol over (2 2 0) facet of ZnAl$_2$O$_4$. The methanol molecule in this case adsorbs on top of the same Al site on which the adsorbate at position 11 also adsorbs (a case of class I). But, adsorption of methanol on top of same surface atom yields two completely different outcomes. While in one case (position 11) we observe very little O−H bond activation, the other case (position 13) represents complete dissociation of the O−H bond in methanol. The difference lies in the relative orientation of the adsorbate with respect to the surface. The effect of orientation of adsorbate wrt surface can be understood better if we compare 8 cases (position 1, 2, 3, 8, 10, 11, 12 and 14) that adsorb on the same Al atom. All these cases share a common Al as their final adsorption site, as can be seen from Fig. 3(b). But the bond activation and adsorption energies for all these cases are not uniform. This is due to the relative orientation of the methanol molecule with respect to the catalyst surface. It must be noted at this point that the activation of an adsorbate over any catalyst surface is a complex problem which depends upon combination of multiple factors like arrangement of atoms
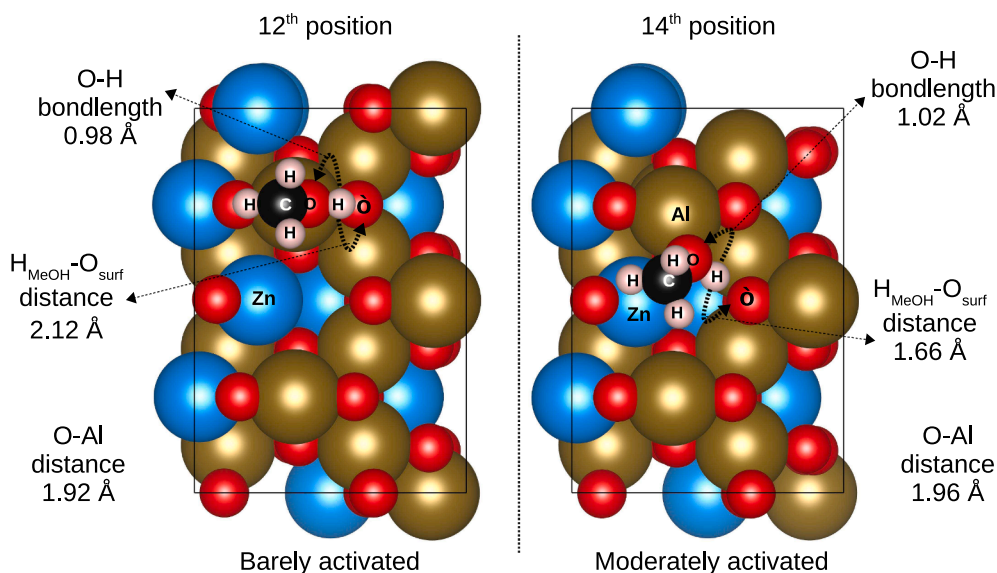
Fig. 4. MeOH is adsorbed at the same site. At 12th position, the OH bond is barely activated whereas at 14th position the OH bond is moderately activated, bringing out the effect of orientation and hence the resulting MeOH surface interaction.
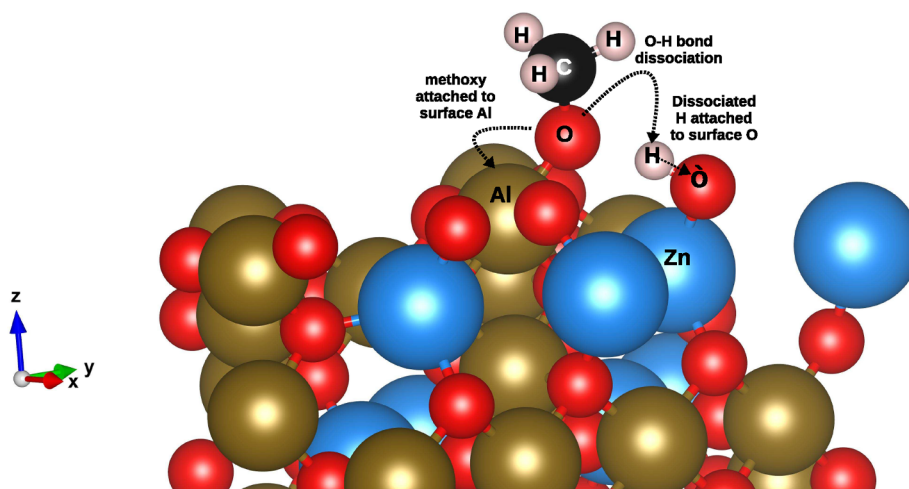

Fig. 5. OH bond dissociation on 220 facet. Surface oxygen atom is marked as Ò. Resultant methoxy group attaches to surface Al atom.

on surface, relative orientation of adsorbate, number of unique sites on surface to name a few. This picture becomes even more complex for a surface of mixed metal oxides like $ZnAl_2O_4$. The possibilities that are needed to be scanned exhaustively become manifold. And hence, bringing out one to one correlation between observed parameters of activation becomes difficult. Nonetheless, our work illustrates the effect that each of these parameters contribute towards understanding adsorption of methanol over $ZnAl_2O_4$. Overall, it is observed that (2 2 0) facet of $ZnAl_2O_4$ exhibits excellent catalytic activity towards an incoming methanol molecule. Al atoms on the surface offer activation of O−H bond in the range of 0.98 Å to 1.04 Å. Complete dissociation of O−H bond indicating spontaneous dissociation over (2 2 0) facet of $ZnAl_2O_4$ was also observed.

3.2. Interaction of MeOH with $ZnAl_2O_4$ (3 1 1) surface

(3 1 1) is a stepped and highly asymmetric surface as shown in Fig. 6. It has all the three elements, viz. Zn, Al, and O on the surface. Like (2 2 0), on (3 1 1) facet also MeOH prefers to be adsorbed via its oxygen pointing towards the surface. Due to asymmetric nature of this stepped surface, it is observed that many more adsorption sites exist as compared to (2 2 0) surface. All possible unique sites on (3 1 1) surface

are scanned to study adsorption of methanol. These sites comprise of top, bridge, and hollow sites with different combinations of Al, Zn, and O. All these initial configurations are shown schematically in Fig. 7(a). The numbers indicate position where MeOH is placed for optimization. Upon relaxation, the final position of MeOH is shown schematically in Fig. 7(b). We report the adsorption energies for methanol on (3 1 1) surface along with various bonds lengths in Table 2.

The same scheme for classification, as used for cases on (2 2 0), is employed to analyze the adsorbed cases on (3 1 1) surface. The adsorbed cases based on O−H bond activation are divided into three classes viz. class I - bare minimum activation of O−H bond (0.98 Å–0.99 Å), class II - higher activation (1.03 Å–1.10 Å), and class III - adsorption on bridge/hollow sites. For (3 1 1) surface it was observed that Zn as well as Al atoms acted as active sites for adsorption with varying strengths. The trend between O−H bond activation and presence of a nearby oxygen atom on surface still holds. The distance of O_{surf} atom from H_{OH} in class I ranges between 1.96 Å and 2.36 Å and the corresponding O−H bond activation is in the range of 0.98 Å–0.99 Å (from initial 0.97 Å). When the distance between O_{surf} and reoriented H_{OH} atom reduces to 1.36 Å–1.58 Å, a greater activation of O−H bond, from 1.03 Å to 1.10 Å, is seen. For the adsorption energies, it is observed that generally the adsorption energies for class II
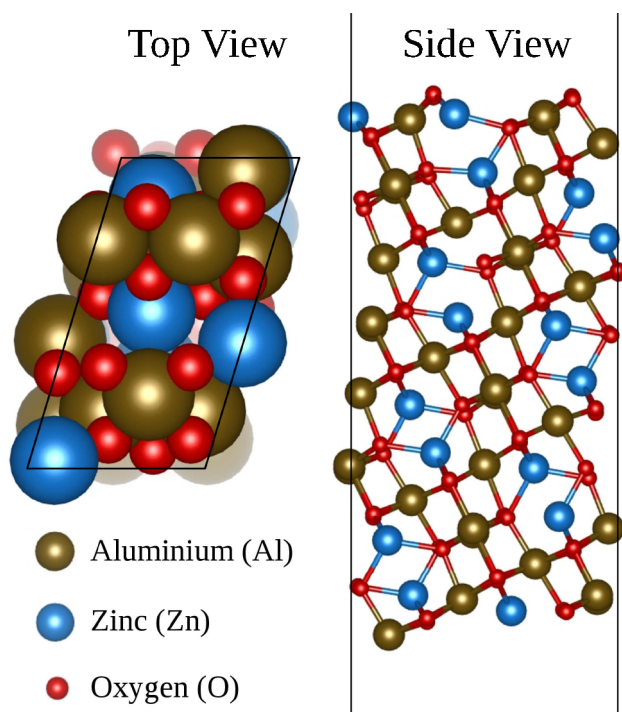
Top View | Side View

- Aluminium (Al)
- Zinc (Zn)
- Oxygen (O)

Fig. 6. The (3 1 1) surface of ZnAl$_2$O$_4$ with the top view and the side view. The (3 1 1) surface has topmost layer composed of Zn, Al and O atoms.

are higher than that of class I. Class III mainly comprises of cases that adsorb at either a bridge or a hollow site and interact mainly via the H$_{OH}$ atom of methanol molecule. The presence of surface oxygen in vicinity explains the bond activation in these cases. However, the adsorption energies for this class are observed to be the least, within 1 eV, when compared with that of other classes.

Interestingly, on (3 1 1) two cases of dissociation are observed viz. one of O−H and other of both O−H and C−H bond dissociation and are shown in Fig. 8-a and b respectively. When the methanol molecule is placed in the vicinity of a surface Zn atom (as seen in 11th position), it dissociated to give away it's H atom to a nearby surface oxygen atom as

shown in Fig. 8-a. The methoxy group after loosing it's H adsorbs on Zn atom. Again the effect that orientation of molecule plays in governing the adsorption can be seen if we compare the cases of 6, 7 (from class II) and 11. We see that methanol when adsorbed on top of same Zn atom (as seen from Fig. 7-b) results into different outcomes, with dissociation of O−H bond in one case (position 11) (see Fig. 8-a), very high activation of O−H bond (O−H bond stretches to 1.10 Å) in the other (position 7), and considerable activation up to 1.03 Å in the third case (position 6). The second case of dissociation (see Fig. 8-b) is even more interesting as it undergoes dissociation of not only O−H bond but also one of the C−H bonds in methanol. It was observed that the methanol molecule first loses it's H$_{OH}$ and further another H connected to C. The adsorption of methanol in this case is not directly on top of any surface atom but instead at a hollow site where both the dissociated H atoms had surface oxygen atoms in the vicinity. After dissociation of two H from methanol, the remaining H$_2$CO group adsorbs on a nearby Al site as shown in Fig. 8-b. This case is particularly very important as it indicates spontaneous dissociation of both O−H and C−H bonds from methanol molecule. We also understand that the observed effect is a combined output of various factors like environment of surface as experienced by methanol, orientation of the adsorbate with respect to the surface, stepped nature of the surface and availability of surface oxygen in the vicinity of the molecule.

3.3. Comparison of (2 2 0) and (3 1 1) bare surfaces

To understand the variation in interaction of MeOH with (2 2 0) and (3 1 1) facets, we have investigated the charge distribution, projected Density of States (pDOS) and atomic arrangement of the bare surfaces. We also report the differential Mulliken charges for surface atoms. On the bare (2 2 0) surface, four Al and eight O atoms exist on the surface, available for interaction with incoming methanol. All Al atoms on the surface are equivalent in terms of environment, charge distribution and have an effective positive charge of 1.67e. Every Al atom is surrounded with four O atoms, one Zn atom and three other Al atoms. Interestingly two types of oxygen atoms exist on the surface. Four out of the eight oxygen atoms on surface are coordinated with three surface Al atoms while the remaining four are coordinated with one surface Al atom and one subsurface Zn atom. The oxygens connected with three Al atoms have a higher negative charge on them, −1.07e. While the ones
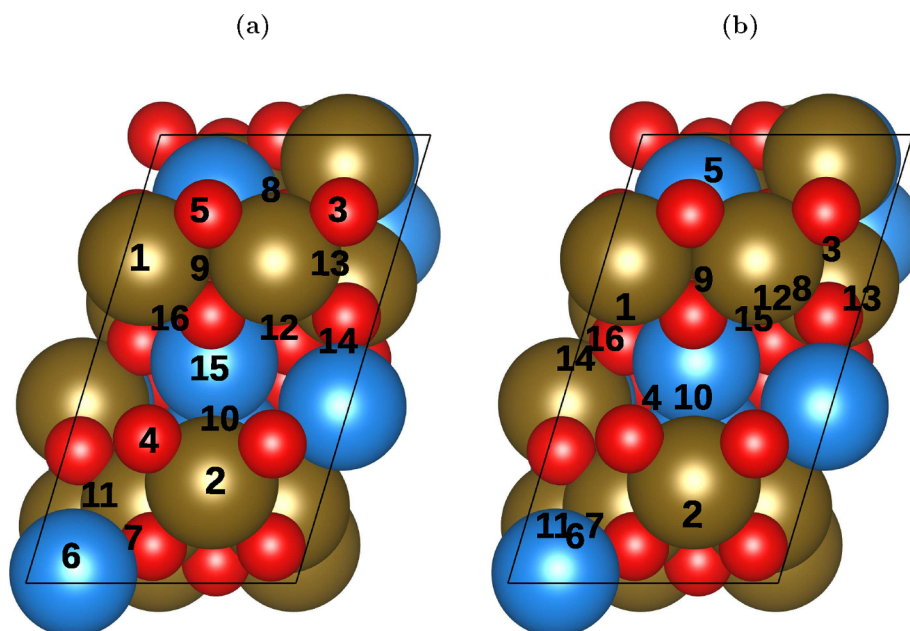
(a)   (b)

Fig. 7. (a) Initial positions of adsorbate on the surface (b) final positions of methanol upon adsorption on (3 1 1) facet.

Table 2

Adsorption energies, O−H bond activation, distance between O_{OH} and surface metal (M) atom, and H_{OH}-O_{surf} distance for adsorption studied at various positions as indicated in Column 1 on (3 1 1).

Adsorption Site	E_{ads} (eV)	O−H bondlengths (Å)	O−M distance (Å)	H_{OH}-O_{surf} distance (Å)
		Class I - Barely activated		
1	−1.1072	0.99	2.03 -Al	1.96
8	−1.2339	0.99	2.02 -Al	2.00
13	−0.8831	0.98	2.05 -Al	2.28
12	−1.2588	0.98	2.02 -Al	2.36
		Class II - Highly activated		
7	−1.3779	1.10	2.01 -Zn	1.36
16	−1.6118	1.04	1.98 -Al	1.55
6	−1.4647	1.03	2.02 -Zn	1.58
2	−0.9155	1.03	2.13 -Al	1.57
		Class III - Adsorbed on bridge/hollow		
10	−0.8264	1.04	3.40 -Al	1.54
14	−0.9464	1.02	2.97 -Zn	1.66
4	−0.7160	1.02	3.74 -Al	1.60
3	−0.4748	0.99	3.53 -Al	1.81
5	−0.4866	0.99	3.93 -Al	1.82
9	−0.5195	0.99	3.10 -Al	1.83

Fig. 9. pDOS plots for two types of surface oxygen atoms on (2 2 0) surface. Charges on each type of oxygen atom is mentioned in the plot. Subscripts on O_{xy} denote the coordination of O atoms, wherein x and y are the number of Al and Zn atoms coordinated with O respectively.

Fig. 10. pDOS plots for three types of surface oxygen atoms on (3 1 1) surface. Charges on each type of oxygen atom is mentioned in the plot. Subscripts on O_{xy} denote the coordination of O atoms, wherein x and y are the number of Al and Zn atoms coordinated with O respectively.

connected with one Zn and one Al have a negative charge of −1.03e. Thus, though Zn is not exposed on the surface, its coordination with surface oxygen changes the nature of oxygen atom on the surface. This difference in the surface oxygen can be seen in the corresponding pDOS plots, shown in Fig. 9. We denote the coordination of O atoms with Al and Zn atoms as O_{xy}, wherein x and y are the number of Al and Zn atoms coordinated with O respectively. Thus, O_{30} represents an oxygen coordinated with 3 Al and 0 Zn whereas O_{11} represents oxygen coordinated with one Al and one Zn. The pDOS plots clearly shows a shift in the peaks of more coordinated oxygen atom (O_{30} - blue) with slightly more negative charge away from the Fermi energy in comparison with the other O (O_{11} - red) that is coordinated with lesser number of atoms on the surface. Lesser coordinated O atom is observed to be lesser negative. Presence of different kinds of atoms with varying charge distribution on the surface is indeed desirable as it would offer more
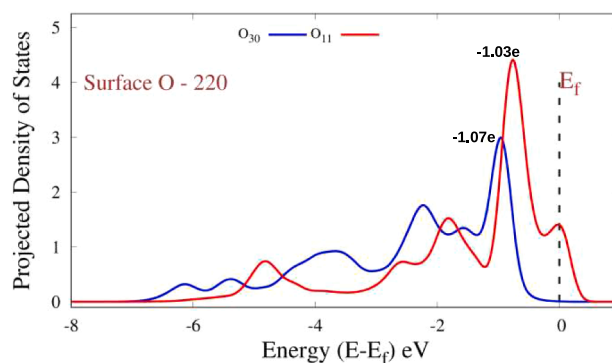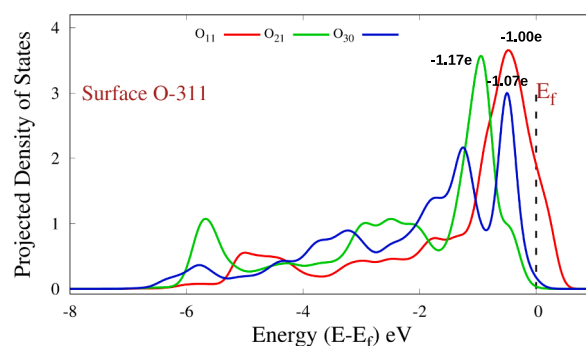
adsorption sites with varying strengths. On (3 1 1) surface, there are four O atoms. Out of these four, two O atoms have differential Mulliken charges of −1.00e and other two with charges −1.07e and −1.17e. Difference in the pDOS signatures can be observed for these O atoms as shown in Fig. 10. The most negatively charged surface oxygen atom
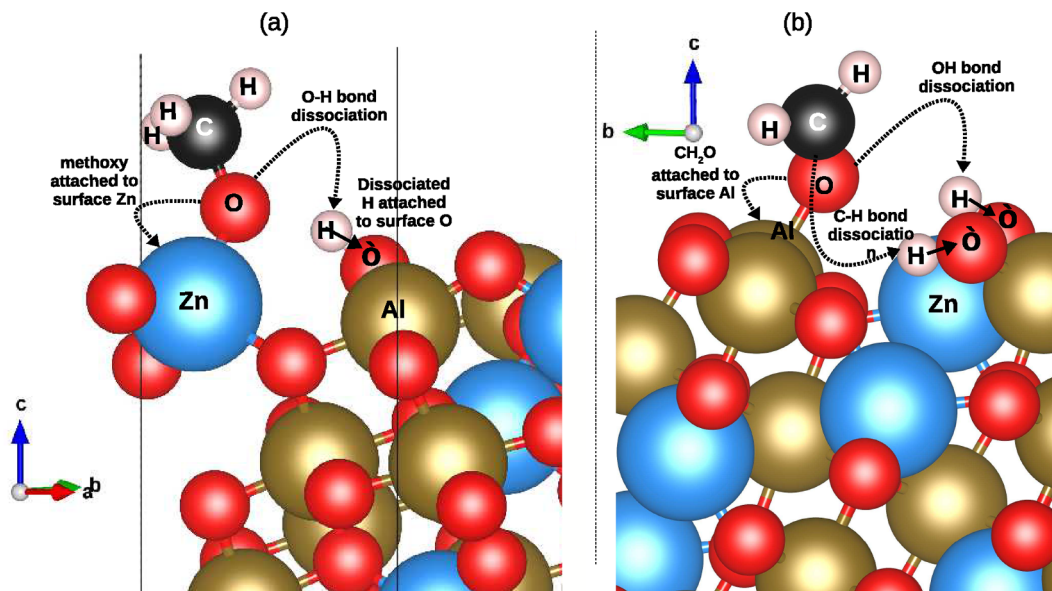

Fig. 8. Spontaneous O−H and C−H bond breaking at 311 facet. Surface oxygen atoms are indicated as Ò. When the active site is Zn(Al), the resultant methoxy group attaches to Zn(Al). The dissociated H atom attaches to surface oxygen atom (Ò).
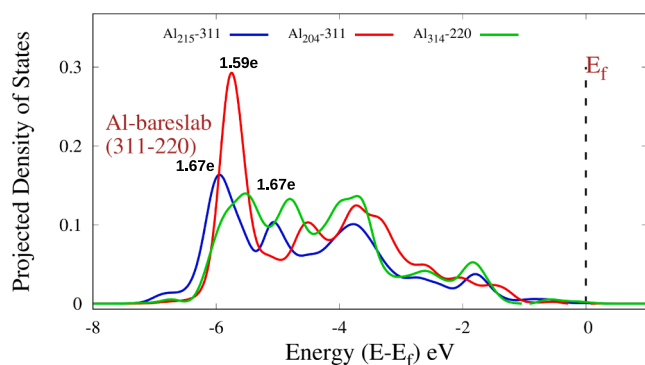
Fig. 11. pDOS plots for Al atoms on (3 1 1) and (2 2 0) surface. Charges on each of the Al atom is mentioned in the plot. Subscripts on Al_{xyz} denote the co-ordination of Al atoms, wherein x, y, and z are the number of Al, Zn, and O atoms coordinated with Al respectively.
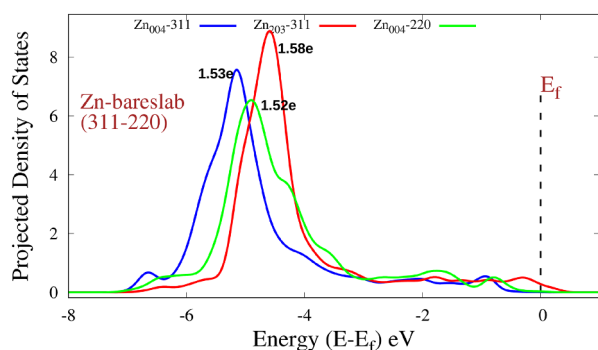

Fig. 12. pDOS plots for Zn atoms on (3 1 1) and (2 2 0) surface. Charge on each of the Zn atom is mentioned in the plot. Subscripts on Zn_{xyz} denote the co-ordination of Zn atoms, wherein x, y, and z are the number of Al, Zn, and O atoms coordinated with Zn respectively.

also turns out to be the most coordinated i.e. coordinated with two Al and one Zn atom (O_{21}-green) with corresponding maximum shift away from the Fermi energy. The other two oxygen atoms also follow the coordination trends wherein the least coordinated O_{11}(in red) is the closest to the Fermi energy followed by O_{30}. Further, there are two kinds of Zn atoms present on the (3 1 1) surface. One is tri-coordinated with oxygen atoms and has a resultant positive charge of 1.53e while the other Zn is tetra-coordinated with oxygen atoms and contains a charge of 1.58e. These surface Zn atoms act as sites that dissociate the O−H from methanol and also act as one of the favorable site for adsorption of methanol. Out of the three Al sites present on the surface, two have effective positive charge of 1.59e and the remaining one with 1.67e. Corresponding pDOS plots for Al and Zn atoms in (2 2 0) and (3 1 1) surface are shown in Fig. 11 and Fig. 12 respectively. A clear redistribution of energy levels can be seen in case of Al atoms over (2 2 0) vs (3 1 1) surface as shown in Fig. 11. The Al_{314} atom on (2 2 0) surface is surrounded with three Al, one Zn, and four oxygen atoms, and the corresponding pDOS (shown in green) is broad and diffuse. On the other hand, pDOS of Al_{204} (in red) and Al_{215} (in blue) atoms on (3 1 1) surface have sharp peaks at around −6 eV. Further, it is interesting to note that though Zn_{004} (in green) on (2 2 0) and Zn_{004} (in blue) on (3 1 1) have almost same charge and number of atoms in the vicinity, their peaks in Fig. 12 are evidently different. This is due to different charges on coordinated oxygen atoms. Hence, indicating that not only the immediate neighbors of an atom but the overall surface geometry plays a role in changing the chemical signatures of an atom on the surface.

Thus overall, we observe that based on Mulliken charge analysis of (2 2 0) and (3 1 1) surface, more variation in the charge distribution is

observed for (3 1 1) surface in comparison with (2 2 0). This variation arises due to the step nature of (3 1 1) surface. Availability of multiple adsorption sites with varying charge distribution is indeed desirable as that allows diffusion of an adsorbate on the catalytic surface. This diffusion is very useful when the adsorbate comes in contact with another reactant. From our adsorption studies for methanol over the two surfaces, we unravel many interesting possibilities of O−H bond activation, O−H bond dissociation and also C−H bond dissociation in methanol. While (2 2 0) demonstrates a case of O−H bond activation, (3 1 1) exhibits its capacity to dissociate both O−H and C−H bonds from methanol. The O−H bond activation on (3 1 1) surface is also observed to be higher in general compared to that of (2 2 0). And hence, we propose that though both surfaces give an excellent catalytic activity towards methanol adsorption, (3 1 1) particularly performs better than (2 2 0). Our work sheds light on various factors that are essential to be considered while studying methanol interaction with mixed metal oxide surface catalysts. Though we do not exhaust all possibilities of methanol adsorption (with respect to changing orientation of methanol over surface), our work points at the immense promise these surfaces hold in terms of not only activating but also dissociating O−H and C−H bonds in methanol without any barrier.

4. Conclusion

Though adsorption of MeOH is extensively studied on varied classes of catalyst, reports of significantly low activation barrier or spontaneous dissociation of O−H as well as C−H bonds of MeOH are very limited. And hence this piece of work on proposed mixed metal oxide as catalyst becomes even more interesting. It is also interesting to note that, proposed mixed metal oxide is in fact a derivative of two commonly used industrial catalyst, Al_2O_3 and ZnO towards MeOH activation. In this work, we illustrate (2 2 0) and (3 1 1) facets of $ZnAl_2O_4$ as excellent candidates for MeOH activation. These two surfaces not only offer significant O−H bond activation but also exhibit one case each of O−H bond dissociation. The dissociation observed in our studies are important as they are spontaneous. To top it, (3 1 1) surface undergoes successive dissociation of one of the C−H bonds as well. In an attempt to understand the factors that influence O−H bond activation/dissociation over any catalyst surface we dwelled deeper into systematically correlating the observed parameters. Availability of surface oxygen in the vicinity of adsorbing methanol is of prime importance. Hence, we can safely say that a surface rich with oxygen atoms of varying charges is desirable for multiple bond activations or even dissociation. Atomic arrangement of atoms on surface turned out to be another important factor in understanding the adsorption energy trends. Coordination of surface atoms and hence availability of sites with variation in charges on the surface unravel the trends in bond activations. Lastly, we propose that (3 1 1) surface offers better catalytic activity than (2 2 0) due to its stepped geometry and availability of inequivalent adsorption sites for interaction with an incoming MeOH. It was observed from the literature that most of the studies were restricted to either (1 1 1) or (1 1 0) planar surfaces. Our work in fact illustrates an upper hand in terms of catalytic activity for stepped surfaces like (3 1 1). Through detailed analysis of various factors that govern MeOH activation over these surface, we unleash a whole new chemical space to be explored in this direction.

CRediT authorship contribution statement

Shweta Mehta: Methodology, Validation, Writing - original draft. **Sheena Agarwal:** Methodology, Validation, Writing - review & editing. **Nivedita Kenge:** Validation. **Siva Prasad Mekala:** Resources. **Vipul Patil:** Resources. **T. Raja:** Funding acquisition. **Kavita Joshi:** Conceptualization, Writing - review & editing, Project administration, Supervision.

Declaration of Competing Interest

The authors declare that they have no known competing financial interests or personal relationships that could have appeared to influence the work reported in this paper.

Acknowledgements

References

[1] Global methanol market, industry analysis, size, share, growth, trends, and forecast 2019-2026, 2019. https://www.marketwatch.com/press-release/global-methanol-market-industry-analysis-size-share-growth-trends-and-forecast-2019-2026-2019-09-27.

[2] https://www.strategyr.com/market-report-methanol-forecasts-global-industry-analysts-inc.asp, 2020.

[3] A. Hamnett, Mechanism and electrocatalysis in the direct methanol fuel cell, Catal. Today 38 (4) (1997) 445–457.

[4] Hansan Liu, Chaojie Song, Lei Zhang, Jiujun Zhang, Haijiang Wang, David P Wilkinson, A review of anode catalysis in the direct methanol fuel cell, J. Power Sources 155 (2) (2006) 95–110.

[5] Robert Schennach, Andreas Eichler, K.D. Rendulic, Adsorption and desorption of methanol on pd (111) and on a pd/v surface alloy, J. Phys. Chem. B 107 (11) (2003) 2552–2558.

[6] O. Rodrıguez de la Fuente, Marta Borasio, Paolo Galletto, Günther Rupprechter, H.-J. Freund, The influence of surface defects on methanol decomposition on pd (111) studied by xps and pm-iras, Surf. Sci. 566 (2004) 740–745.

[7] Marta Borasio, Oscar Rodríguez de la Fuente, Günther Rupprechter, Hans-Joachim Freund, In situ studies of methanol decomposition and oxidation on pd (111) by pm-iras and xps spectroscopy, J. Phys. Chem. B 109 (38) (2005) 17791–17794.

[8] Janine Lichtenberger, Doohwan Lee, Enrique Iglesia, Catalytic oxidation of methanol on pd metal and oxide clusters at near-ambient temperatures, Phys. Chem. Chem. Phys. 9 (35) (2007) 4902–4906.

[9] B.G. Frederick, G. Apai, T.N. Rhodin, Defect structure of clean and chlorinated aluminum oxide films probed by methanol chemisorption, Surf. Sci. 277 (3) (1992) 337–350.

[10] C.T. Au, W. Hirsch, W. Hirschwald, Adsorption and interaction of methanol with zinc oxide: Single crystal faces and zinc oxide-copper catalyst surfaces studied by photoelectron spectroscopy (xps and ups), Surf. Sci. 221 (1–2) (1989) 113–130.

[11] Samia Ilias, Aditya Bhan, Mechanism of the catalytic conversion of methanol to hydrocarbons, ACS Catal. 3 (1) (2012) 18–31.

[12] Xu. Mingting, Jack H Lunsford, D. Wayne Goodman, Alak Bhattacharyya, Synthesis of dimethyl ether (dme) from methanol over solid-acid catalysts, Appl. Catal. A: Gen. 149 (2) (1997) 289–301.

[13] Siranush S. Akarmazyan, Paraskevi Panagiotopoulou, Anastasios Kambolis, Christina Papadopoulou, Dimitris I. Kondarides, Methanol dehydration to dimethylether over al2o3 catalysts, Appl. Catal. B: Environ. 145 (2014) 136–148.

[14] X. Bao, M. Muhler, B. Pettinger, R. Schlögl, G. Ertl, On the nature of the active state of silver during catalytic oxidation of methanol, Catal. Lett. 22 (3) (1993) 215–225.

[15] Jinlong Gong, David W. Flaherty, Rotimi A. Ojifinni, John M. White, C. Buddie Mullins, Surface chemistry of methanol on clean and atomic oxygen pre-covered au (111), J. Phys. Chem. C 112 (14) (2008) 5501–5509.

[16] Sanket K. Desai, Matthew Neurock, K. Kourtakis, A periodic density functional theory study of the dehydrogenation of methanol over pt (111), J. Phys. Chem. B 106 (11) (2002) 2559–2568.

[17] Sung Sakong, Axel Groß, Density functional theory study of the partial oxidation of methanol on copper surfaces, J. Catal. 231 (2) (2005) 420–429.

[18] Øyvind Borck, Elsebeth Schröder, First-principles study of the adsorption of methanol at the α -al2o3 (0001) surface, J. Phys. Condens. Matter 18 (1) (2005) 1–12.

[19] Alejandro Montoya, Brian S Haynes, Methanol and methoxide decomposition on silver, J. Phys. Chem. C 111 (27) (2007) 9867–9876.

[20] N. Donghai Mei, Aaron Deskins, Michel Dupuis, Qingfeng Ge, Density functional theory study of methanol decomposition on the ceo2 (110) surface, J. Phys. Chem. C 112 (11) (2008) 4257–4266.

[21] Jaime Oviedo, Rocío Sánchez-de Armas, Miguel Angel San Miguel, Javier F. Sanz, Methanol and water dissociation on tio2 (110): the role of surface oxygen, J. Phys. Chem. C 112 (46) (2008) 17737–17740.

[22] Raj Ganesh S. Pala, Horia Metiu, Selective promotion of different modes of methanol adsorption via the cation substitutional doping of a zno (101̄0) surface, J. Catal. 254 (2) (2008) 325–331.

[23] Ruibin Jiang, Wenyue Guo, Ming Li, Fu. Dianling, Honghong Shan, Density functional investigation of methanol dehydrogenation on pd (111), J. Phys. Chem. C 113 (10) (2009) 4188–4197.

[24] Sandra Sá, Hugo Silva, Lúcia Brandão, José M. Sousa, Adélio Mendes, Catalysts for methanol steam reforming–a review, Appl. Catal. B: Environ. 99 (1–2) (2010) 43–57.

[25] Solange R. Blaszkowski, Rutger A. van Santen, Theoretical study of c- c bond formation in the methanol-to-gasoline process, J. Am. Chem. Soc. 119 (21) (1997) 5020–5027.

[26] Mehdi D. Esrafili, Leila Dinparast, The selective adsorption of formaldehyde and methanol over al-or si-decorated graphene oxide: A dft study, J. Mol. Graph. Model. 80 (2018) 25–31.

[27] Do Hwan Kim, Sung-Soo Bae, Suklyun Hong, Sehun Kim, Atomic and electronic structure of methanol on ge(100), Surf. Sci. 604 (2) (2010) 129–135.

[28] Jan Andzelm, Niranjan Govind, George Fitzgerald, Amitesh Maiti, Dft study of methanol conversion to hydrocarbons in a zeolite catalyst, Int. J. Quant. Chem. 91 (3) (2003) 467–473.

[29] Rajiv Shah, Julian D. Gale, Michael C. Payne, Methanol adsorption in zeolites a first-principles study, J. Phys. Chem. 100 (28) (1996) 11688–11697.

[30] Ch Ammon, A. Bayer, G. Held, B. Richter, Th. Schmidt, H.-P. Steinrück, Dissociation and oxidation of methanol on cu (110), Surf. Sci. 507 (2002) 845–850.

[31] Qiang Sun, Bairong Shen, Kangnian Fan, Jingfa Deng, Roles of surface and subsurface oxygen in the dehydrogenation of methanol on silver surface, Chem. Phys. Lett. 322 (1–2) (2000) 1–8.

[32] Xu. Bingjun, Jan Haubrich, Thomas A. Baker, Efthimios Kaxiras, Cynthia M. Friend, Theoretical study of o-assisted selective coupling of methanol on au (111), J. Phys. Chem. C 115 (9) (2011) 3703–3708.

[33] Wen-Kai Chen, Shu-Hong Liu, Mei-Juan Cao, Qian-Gu Yan, Lu. Chun-Hai, Adsorption and dissociation of methanol on au (1 1 1) surface: A first-principles periodic density functional study, J. Mol. Struct. THEOCHEM 770 (1–3) (2006) 87–91.

[34] Yasuyuki Ishikawa, Meng-Sheng Liao, Carlos R. Cabrera, Oxidation of methanol on platinum, ruthenium and mixed pt–m metals (m = ru, sn): a theoretical study, Surf. Sci. 463 (1) (2000) 66–80.

[35] C.J. Zhang, P. Hu, A first principles study of methanol decomposition on pd (111): mechanisms for o–h bond scission and c–o bond scission, J. Chem. Phys. 115 (15) (2001) 7182–7186.

[36] Gui-Chang Wang, Yu-Hua Zhou, Yoshitada Morikawa, Junji Nakamura, Zun-Sheng Cai, Xue-Zhuang Zhao, Kinetic mechanism of methanol decomposition on ni (111) surface: a theoretical study, J. Phys. Chem. B 109 (25) (2005) 12431–12442.

[37] Yu-Hua Zhou, Pei-Hong Lv, Gui-Chang Wang, Dft studies of methanol decomposition on on ni (1 0 0) surface: compared with ni (1 1 1) surface, J. Mol. Catal. A: Chem. 258 (1–2) (2006) 203–215.

[38] Susumu Yanagisawa, Takao Tsuneda, Kimihiko Hirao, Yoichi Matsuzaki, Theoretical investigation of adsorption of organic molecules onto fe (110) surface, J. Mol. Struct. THEOCHEM 716 (1–3) (2005) 45–60.

[39] Ruibin Jiang, Wenyue Guo, Ming Li, Houyu Zhu, Lianming Zhao, Lu. Xiaqing, Honghong Shan, Methanol dehydrogenation on rh (1 1 1): A density functional and microkinetic modeling study, J. Mol. Catal. A: Chem. 344 (1–2) (2011) 99–110.

[40] Minhua Zhang, Wu. Xingyu, Yu. Yingzhe, A comparative dft study on the dehydrogenation of methanol on rh (100) and rh (110), Appl. Surf. Sci. 436 (2018) 268–276.

[41] Ana S Moura, Jose LC Fajín, Ana SS Pinto, Marcos Mandado, M. Natalia, D.S. Cordeiro, Competitive paths for methanol decomposition on ruthenium: A dft study, J. Phys. Chem. C 119 (49) (2015) 27382–27391.

[42] Maria Marta Branda, Patricia Gabriela Belelli, R.M. Ferullo, Norberto Jorge Castellani, Proton abstraction ability of mgo: a dft cluster model study of the role of surface geometry, Catal. Today 85 (2–4) (2003) 153–165.

[43] Lawrence T. Sein Jr, Susan A. Jansen, Dft study of the adsorption and dissociation of methanol on nial (100), J. Catal. 196 (2) (2000) 207–211.

[44] Orest Skoplyak, Carl A. Menning, Mark A. Barteau, Jingguang G. Chen, Experimental and theoretical study of reactivity trends for methanol on co/ pt (111) and ni/ pt (111) bimetallic surfaces, J. Chem. Phys. 127 (11) (2007) 114707.

[45] Valeria Orazi, P. Bechthold, Paula Verónica Jasen, R. Faccio, Maria Estela Pronsato, Estela Andrea Gonzalez, Dft study of methanol adsorption on ptco (111), Appl. Surf. Sci. 420 (2017) 383–389.

[46] Øyvind Borck, Ingeborg-Helene Svenum, Anne Borg, Adsorption of methanol and methoxy on nial (1 1 0) and ni3al (1 1 1): A dft study, Surf. Sci. 603 (16) (2009) 2378–2386.

[47] Pan Du, Ping Wu, Chenxin Cai, Mechanism of methanol decomposition on the pt3ni (111) surface: Dft study, J. Phys. Chem. C 121 (17) (2017) 9348–9360.

[48] Mehdi D. Esrafili, Roghaye Nurazar, A dft study on the possibility of using boron nitride nanotubes as a dehydrogenation catalyst for methanol, Appl. Surf. Sci. 314 (2014) 90–96.

[49] Carolina Pistonesi, Alfredo Juan, Arnold Péter Farkas, F. Solymosi, Dft study of methanol adsorption and dissociation on β -mo2c (0 0 1), Surface Sci. 602(13) (2008) 2206–2211.

[50] Gregory K. Smith, Sen Lin, Wenzhen Lai, Abhaya Datye, Daiqian Xie, Hua Guo, Initial steps in methanol steam reforming on pdzn and zno surfaces: Density functional theory studies, Surf. Sci. 605 (7–8) (2011) 750–759.

[51] M.M. Branda, J.E. Peralta, N.J. Castellani, R.H. Contreras, Theoretical study of charge transfer interactions in methanol adsorbed on magnesium oxide, Surf. Sci. 504 (2002) 235–243.

[52] Øyvind Borck, Elsebeth Schröder, Adsorption of methanol and methoxy on the α -cr2o3 (0001) surface, J. Phys. Condens. Matter 18 (48) (2006) 10751–10763.

[53] Zhang Riguang, Liu Hongyan, Ling Lixia, Li Zhong, Wang Baojun, A dft study on the formation of ch3o on cu2o (1 1 1) surface by ch3oh decomposition in the absence or presence of oxygen, Appl. Surf. Sci. 257 (9) (2011) 4232–4238.

[54] R. Sanchez de Armas, J. Oviedo, M.A. San Miguel, J.F. Sanz, Methanol adsorption

and dissociation on tio2 (110) from first principles calculations, J. Phys. Chem. C 111 (27) (2007) 10023–10028.

[55] Weijia Liu, Jian-guo Wang, Xiaojing Guo, Wei Fang, Mingjie Wei, Lu. Xiaohua, Lu. Linghong, Dissociation of methanol on hydroxylated tio2-b (1 0 0) surface: Insights from first principle dft calculation, Catal. Today 165 (1) (2011) 32–40.

[56] Dianhua Liu, Chunfeng Yao, Jianqiang Zhang, Dingye Fang, Dasheng Chen, Catalytic dehydration of methanol to dimethyl ether over modified γ -al2o3 catalyst, Fuel 90 (5) (2011) 1738–1742.

[57] Cong T. Vo, Lam K. Huynh, J.-Y. Hung, Jyh-Chaing Jiang, Methanol adsorption and decomposition on zno (1010̄) surface: A density functional theory study, Appl. Surf. Sci. 280 (2013) 219–224.

[58] María M. Branda, Graciela R. Garda, Horacio A. Rodriguez, Norberto J. Castellani, Methanol decomposition on the β-ga2o3 (1 0 0) surface: A dft approach, Appl. Surf. Sci. 254 (1) (2007) 120–124.

[59] Marçal Capdevila-Cortada, Max García-Melchor, Núria López, Unraveling the structure sensitivity in methanol conversion on ceo2: A dft+ u study, J. Catal. 327 (2015) 58–64.

[60] N. Donghai Mei, Aaron Deskins, Michel Dupuis, Qingfeng Ge, Methanol adsorption on the clean ceo2 (111) surface: A density functional theory study, J. Phys. Chem. C 111 (28) (2007) 10514–10522.

[61] Zhao Liu, Charles C. Sorrell, Pramod Koshy, Judy N. Hart, Dft study of methanol adsorption on defect-free ceo2 low-index surfaces, ChemPhysChem 20 (16) (2019) 2074–2081.

[62] Chengwu Yang, Fabian Bebensee, Alexei Nefedov, Christof Wöll, Thomas Kropp, Leonid Komissarov, Christopher Penschke, Robin Moerer, Joachim Paier, Joachim Sauer, Methanol adsorption on monocrystalline ceria surfaces, J. Catal. 336 (2016) 116–125.

[63] Walter G. Reimers, Maria M. Branda, Methanol decomposition on low index and stepped ceo2 surfaces from gga+ u, Appl. Surf. Sci. 394 (2017) 509–518.

[64] Maria Marta Branda, R.M. Ferullo, Patricia Gabriela Belelli, Norberto Jorge Castellani, Methanol adsorption on magnesium oxide surface with defects: a dft study, Surf. Sci. 527 (1–3) (2003) 89–99.

[65] Hugo Petitjean, Konstantin Tarasov, Francoise Delbecq, Philippe Sautet, Jean Marc Krafft, Philippe Bazin, Maria Cristina Paganini, Elio Giamello, Michel Che, Helene Lauron-Pernot, et al., Quantitative investigation of mgo brønsted basicity: Dft, ir, and calorimetry study of methanol adsorption, J. Phys. Chem. C, 114(7) (2010) 3008–3016.

[66] S. Bocanegra, A. Ballarini, P. Zgolicz, O. Scelza, S. De Miguel, Highly selective and stable bimetallic catalysts supported on different materials for n-butane dehydrogenation, Catal. Today 143 (3–4) (2009) 334–340.

[67] Janina Okal, Mirosław Zawadzki, Combustion of propane over novel zinc aluminate-supported ruthenium catalysts, Appl. Catal. B: Environ. 105 (1–2) (2011) 182–190.

[68] Qianhe Liu, Lei Wang, Congxin Wang, Qu. Wei, Zhijian Tian, Huaijun Ma, Donge Wang, Bingchun Wang, Xu. Zhusheng, The effect of lanthanum doping on activity of zn-al spinel for transesterification, Appl. Catal. B: Environ. 136 (2013) 210–217.

[69] Suellen Battiston, Caroline Rigo, Eric da Cruz Severo, Marcio Antonio Mazutti, Raquel Cristine Kuhn, André Gündel, Edson Luiz Foletto, Synthesis of zinc aluminate (znal2o4) spinel and its application as photocatalyst, Mater. Res. 17(3) (2014) 734–738.

[70] H.P. de Macedo, R.L.B. de A. Medeiros, A.L. de Medeiros, A.A.S. de Oliveira, G.P. de Figueredo, M.A. de F. Melo, and D.M. de A. Melo, Characterization of ZnAl2O4 spinel obtained by hydrothermal and microwave assisted combustion method: a comparative study, Mater. Res. 20 (2017) 29–33.

[71] P.E. Blöchl, Projector augmented-wave method, Phys. Rev. B 50 (24) (1994) 17953–17979.

[72] G. Kresse, D. Joubert, From ultrasoft pseudopotentials to the projector augmented-wave method, Phys. Rev. B 59 (3) (1999) 1758–1775.

[73] John P. Perdew, Kieron Burke, Matthias Ernzerhof, Generalized gradient approximation made simple, Phys. Rev. Lett. 77 (18) (1996) 3865–3868.

[74] John P. Perdew, Kieron Burke, Matthias Ernzerhof, Generalized gradient approximation made simple [phys. rev. lett. 77, 3865 (1996)], Phys. Rev. Lett. 78(7) (1997) 1396–1396.

[75] G. Kresse, J. Hafner, *Ab initio* molecular-dynamics simulation of the liquid-metal–amorphous-semiconductor transition in germanium, Phys. Rev. B 49 (20) (1994) 14251–14269.

[76] G. Kresse, J. Furthmüller, Efficient iterative schemes for *ab initio* total-energy calculations using a plane-wave basis set, Phys. Rev. B 54 (16) (1996) 11169–11186.

[77] G. Kresse, J. Furthmüller, Efficiency of ab-initio total energy calculations for metals and semiconductors using a plane-wave basis set, Comput. Mater. Sci. 6 (1) (1996) 15–50.

[78] Anubhav Jain, Shyue Ping Ong, Geoffroy Hautier, Wei Chen, William Davidson Richards, Stephen Dacek, Shreyas Cholia, Dan Gunter, David Skinner, Gerbrand Ceder, et al., Commentary: The materials project: A materials genome approach to accelerating materials innovation, Appl. Materi. 1(1) (2013) 011002.

[79] Shyue Ping Ong, William Davidson Richards, Anubhav Jain, Geoffroy Hautier, Michael Kocher, Shreyas Cholia, Dan Gunter, Vincent L. Chevrier, Kristin A. Persson, Gerbrand Ceder, Python materials genomics (pymatgen): A robust, open-source python library for materials analysis, Comput. Mater. Sci. 68 (2013) 314–319.

[80] Richard Dronskowski, Peter E Blöchl, Crystal orbital hamilton populations (cohp): energy-resolved visualization of chemical bonding in solids based on density-functional calculations, J. Phys. Chem. 97 (33) (1993) 8617–8624.

[81] Volker L. Deringer, Andrei L. Tchougréeff, Richard Dronskowski, Crystal orbital Hamilton population (cohp) analysis as projected from plane-wave basis sets, J. Phys. Chem. A 115 (21) (2011) 5461–5466.

[82] Stefan Maintz, Volker L. Deringer, Andrei L. Tchougréeff, Richard Dronskowski, Analytic projection from plane-wave and paw wavefunctions and application to chemical-bonding analysis in solids, J. Comput. Chem. 34 (29) (2013) 2557–2567.

[83] Stefan Maintz, Volker L. Deringer, Andrei L. Tchougréeff, Richard Dronskowski, Lobster: A tool to extract chemical bonding from plane-wave based dft, J. Comput. Chem. 37 (11) (2016) 1030–1035.

[84] Atsuto Seko, Koretaka Yuge, Fumiyasu Oba, Akihide Kuwabara, Isao Tanaka, Prediction of ground-state structures and order-disorder phase transitions in ii–iii spinel oxides: A combined cluster-expansion method and first-principles study, Phys. Rev. B 73 (18) (2006) 184117.

[85] M.A. Lahmer, First-principles study of the structural, electronic, and optical properties of the clean and o-deficient znal2o4 (110) surfaces, Surf. Sci. 677 (2018) 105–114.